

Learning to combine top-down context and feed-forward representations under ambiguity with apical and basal dendrites

Nizar Islah^{1,3*}, Guillaume Etter^{1,2,3*}, Mashbayar Tugsbayar^{2,3,*}, Tugce Gurbuz^{1,2},
Blake Richards^{2,3}, Eilif Muller^{1,3}

December 12, 2023

1 - Université de Montréal, CHU Ste-Justine Research Center (Architectures of Biological Learning Lab), Montréal, Canada

2 - McGill University, Montréal, Canada

3 - Mila Quebec AI Institute, Montréal, Canada

* - equal contribution

Abstract

One of the most striking features of neocortical anatomy is the presence of extensive top-down projections into primary sensory areas. Notably, many of these top-down projections impinge on the distal apical dendrites of pyramidal neurons, where they exert a modulatory effect, altering the gain of responses. It is thought that these top-down projections carry contextual information that can help animals to resolve ambiguities in sensory data. However, it has yet to be demonstrated how such modulatory connections to the distal apical dendrites can serve this computational function. Here, we develop a computational model of pyramidal cells that integrates contextual information from top-down projections to apical compartments with sensory representations driven by bottom-up projections to basal compartments. When input stimuli are ambiguous and relevant contextual information is available, the apical feedback modulates the basal signals to recover unambiguous sensory representations. Importantly, when stimuli are unambiguous, contextual information which is irrelevant or opposes sensory evidence is appropriately ignored by the model. By generalizing the task to temporal sequences, we further show that our model can learn to integrate contextual information across time. Using layer-wise relevance propagation, we extract the importance of individual neurons to the prediction of each category, revealing that neurons that are most relevant for the overlap of categories receive the largest magnitude of top-down signals, and are necessary for solving the task. This work thus provides a proof-of-concept demonstrating how the top-down modulatory inputs to apical dendrites in sensory regions could be used by the cortex to handle the ambiguities that animals encounter in the real world.

1 Introduction

Accurate perception relies on appropriate integration of context, as sensory signals contain incomplete or ambiguous information (Mumford, 1992; R. P. N. Rao & Ballard, 1999). Contextual information can be derived from a number of sources, including the spatial and temporal domains (Eichenbaum, 2017), task demands (Gilbert & Li, 2013), as well as other sensory modalities.

Several key neuroanatomical and cellular features could support the computations associated with context integration. In the mammalian brain, context has been proposed to be conveyed by top-down feedback pathways which are abundant in sensory regions of the neocortex (Felleman & Van Essen, 1991; Harris et al., 2019; Markov et al., 2014). Perturbations of top-down pathways from higher order areas have been associated with delayed object recognition (Kar & DiCarlo, 2021) as well as disrupted stimulus response curves in lower-order regions (Nassi et al., 2013; Wang et al., 2007), which may reflect deficits in contextual processing. Several feed-forward computational models of perception have implemented top-down pathways to enable object recognition of occluded images (George et al., 2017; Spoerer et al., 2017) as well as context-invariant perception (Naumann et al., 2022).

In the neocortex, pyramidal neurons are thought to integrate feedforward and top-down, feedback information at their basal and apical dendrites, respectively (M. E. Larkum et al., 2007; Spruston, 2008). Notably, feedback has been proposed to modulate rather than drive neuronal activities (Sherman & Guillery, 1998). This idea is supported by the unique morphological and physiological properties of pyramidal neurons, as activity in apical dendrites in vivo is generally not sufficient to drive somatic output responses alone (Jarvis et al., 2018; M. Larkum, 2013; M. E. Larkum et al., 1999; Stuart & Spruston, 1998). On the other hand, activation of the apical compartment has been shown to act as a gain modulator, amplifying concurrent basal activity (M. E. Larkum et al., 2004). While the physiological properties of pyramidal neurons have been described extensively (see Spruston (2008) for review), there is no consensus on the exact mechanism by which top-down signals from higher-order regions modulate somatic firing rates and update sensory representations.

Here, we propose a functional model that learns to use context only when such information is relevant, and ignores it otherwise, ultimately learning a useful mapping of top-down contextual information onto apical compartments. We examine character recognition tasks in cases where the characters are ambiguous and consider two different computational settings. First, the contextual representation is directly given to the model which learns to use this top-down input to resolve the ambiguities. Then, the representation of context is learned, from the temporal framing of the character in words or sequences of digits. In both settings, we show that the model learns to use apical modulation, driven by contextual inputs, to resolve sensory ambiguities. We find that a Hadamard (element-wise multiplicative) dendritic integration rule informed by physiological data enables strong performance in both settings of the task.

To gain insights into the learned mechanisms of top-down modulation involved in our model, we applied layer-wise relevance propagation (Bach et al., 2015) to identify the relative contributions of individual neurons and their apical compartments to network function. We identified a subset of neurons that are highly relevant for class-pairs which are selectively amplified by top-down signals arriving at their apical dendrites. We propose that, in principle, the representation of context can be learned independently from the impact that it has on ambiguity resolution. These findings provide a candidate mechanism for how neocortical pyramidal neurons integrate top-down contextual information at their apical dendrites to support robust perception in the face of ambiguous data.

2 Results

2.1 Functional model of context integration in apical dendrites

To model how apical dendrites integrate context to refine perceptual representations, we developed a task where correct classification of ambiguous characters requires appropriate integration of contextual cues (Fig. 1a). In this task, we trained a generative model to construct a dataset of ambiguous handwritten digits and letters based on MNIST and EMNIST, respectively. This generative model synthesizes images that are ambiguous between pairs of classes (see Methods). The resulting ambiguity was empirically quantified with a linear classifier trained on unambiguous images (fig. 1b). Inspired by anatomical features of pyramidal neurons, we next developed a model that implements distinct dendritic compartments, a basal compartment for integrating sensory information and an apical compartment for integrating contextual information (Fig. 1c). In the model, a population of n pyramidal neurons has two sources of inputs, represented as vectors: a set of basal inputs, $\mathbf{b} = [b_1, \dots, b_n]$, representing the sensory stream, and a set of apical inputs, $\mathbf{a} = [a_1, \dots, a_n]$, representing the top-down stream. Input images, \mathbf{x} , are encoded by a pretrained network f , with parameters Θ_b . f is a convolutional neural network reflecting initial stages of sensory processing (see Methods for more details on how the encoder is pretrained). The output of $f(x)$ is the basal vector \mathbf{b} .

The firing rate of pyramidal neurons, $\mathbf{h} = [h_1, \dots, h_n]$, is then determined by a thresholded element-wise (neuron-wise) combination of the basal and apical input vectors:

$$\mathbf{h} = \sigma(\mathbf{b}) \odot (\sigma(\mathbf{a}) + 1), \quad (1)$$

where \odot is an element-wise multiplication and σ is the rectified linear unit (ReLU) activation function. We refer to this integration rule as 'Hadamard'. As can be seen from equation 1, the impact of the apical input vector, \mathbf{a} , on the firing rate, \mathbf{h} , is determined by $\sigma(\mathbf{a}) + 1$, which has elements that are by design always greater than or equal to one. As such, the apical activity serves as a thresholded

neuron-wise gain modulator of the basal activity. This modulated basal activity is ultimately the firing rate of the modelled neurons, in-line with previous experimental findings (Waters et al., 2003). Under these constraints, apical inputs affect neuronal activity only under the condition that they exceed their activation threshold (when $a > 0$), similar to the requirement for regenerative calcium spikes for apical inputs to influence somatic spiking in real pyramidal neurons (M. E. Larkum et al., 1999). The output of the model is read-out from a feedforward linear transformation of the pyramidal neurons firing rates:

$$\mu = \mathbf{U}\mathbf{h}, \quad (2)$$

where

$$\mathbf{U}$$

is a pretrained linear transformation and μ represents a higher-order neuronal population. To obtain the apical inputs \mathbf{a} , the context, \mathbf{c} , (which is either derived from temporal context, or given directly, see below) is merged with the output and mapped onto the apical compartment using a multilayer perceptron (MLP), $g(\cdot)$, as follows:

$$\mathbf{a} = g(\mathbf{c} \oplus \mathbf{U}\sigma(\mathbf{b})), \quad (3)$$

where \oplus is the concatenation operation, σ is the ReLU activation, and g is a 2-layer MLP (1 hidden layer) with learnable parameters denoted by Θ_a . The model must use the combination of context and input to determine the representation of both ambiguous and unambiguous characters. For ambiguous characters, which are a mixture of two categories, the readout of the representations of the model will yield two plausible interpretations (one corresponding to the target category, and one corresponding to the contradictory category). The contradictory category refers to the class that induces the most confounding readout classification. Categories other than the target or contradictory we refer to as irrelevant categories. To test whether the model can learn useful apical modulations, we trained the synaptic weights Θ_a with the objective L of modulating basal representations to match the target latent representations under various scenarios of input and context by gradient descent; Fig. 1e; pseudocode 1, and 5) This setup ensures that the top-down model is trained on both unambiguous and ambiguous samples, and that the model must learn to provide the appropriate modulatory signal only when it is relevant, ensuring that our model could learn to ignore contextual information when appropriate. This implementation reflects the fact that, in the mammalian brain, top-down modulation is available from multiple sources and present regardless of whether the sensory inputs are ambiguous or not, and whether the contextual sources are helpful for resolving ambiguity or not.

This suggests an approach where the problem of contextual integration is broken into two parts: (1) how apical dendrites locally learn to use contextual representations c to solve the task and (2) how those contextual representations c can be learned from the temporal frame.

For the first part, our initial experiments assume that context, c , is given in the form of a one-hot vector, a scenario we refer to as the 'oracle context' (see Methods). Subsequent experiments for the second part address the problem of learning a representation of context, c , taking inspiration from the neocortex, where context is, in part, represented by higher-order regions with broader windows of temporal integration (Eichenbaum, 2017) (Fig. 1c; see Methods).

2.2 Resolving ambiguity in the oracle context

To first test if our model can categorize digits under contextual input represented as a one-hot vector (oracle context), we trained g on the ambiguous MNIST/EMNIST task with a loss including all 5 scenarios of stimulus and context (see Methods). We assessed performance of the model in each scenario as the held-out test set accuracy on the pretrained category readout. and found model performance was significantly modulated by top-down signals (one-way ANOVA; $F_4 = 10076.598$; $p < 0.0001$; $n = 313$ independent samples). Test set accuracy on ambiguous digits was $44.619 \pm 8.073\%$ without top-down modulation, and became significantly higher with top-down modulation ($99.491 \pm 1.306\%$; Tukey's test; $p < 0.0001$) if context was matching, but did not improve performance if context was irrelevant (43.920 ± 8.160 ; Tukey's test; $p = 0.4651$; $n = 313$ independent replicates; Fig. 2a; Table 1).

Importantly, the model did not learn to rely solely on top-down context, since performance for unambiguous input and contradictory context remained high (Fig. 2a; 1). To visualize the ability of our model to disambiguate on a population level, we projected the model output μ onto a two-dimensional manifold using t-SNE (Maaten, 2008; Fig. 2b). Ambiguous images that were initially

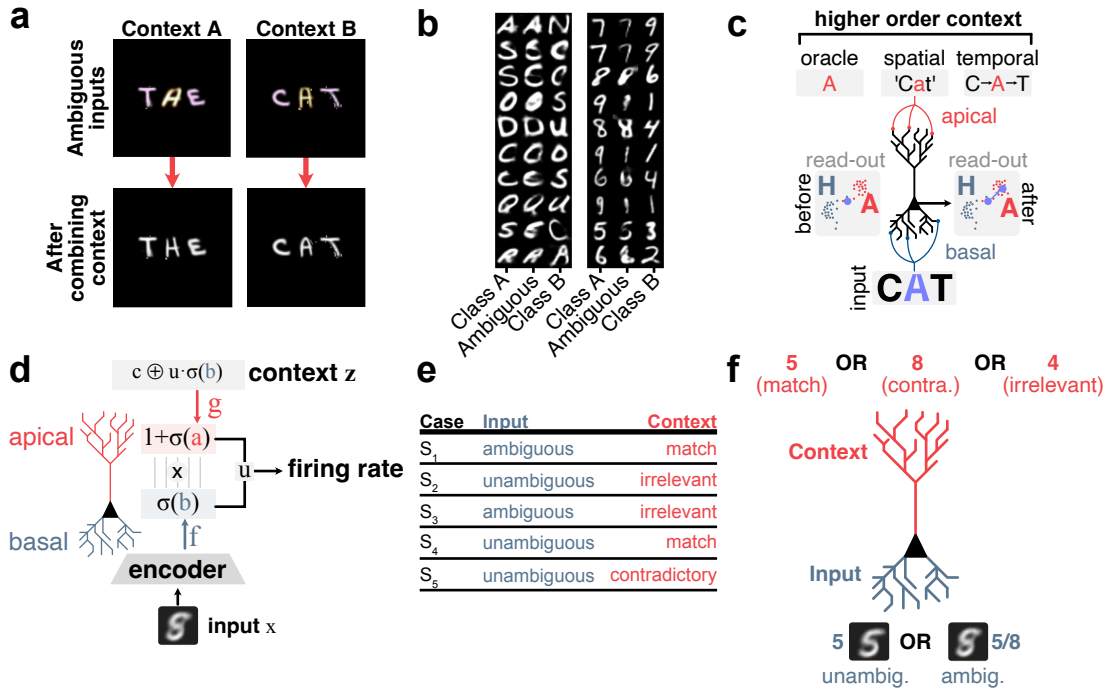


Figure 1: **Functional model of context integration in apical dendrites.** **a**, in our experimental paradigm, ambiguous characters (in yellow, top panels) are resolved by combining context signals (bottom panels). **b**, examples of unambiguous pairs and resulting ambiguous characters generated using EMNIST (left) and MNIST (right). **c**, model of pyramidal neurons with distinct dendritic compartments trained to solve a task of perceptual ambiguity. Before top-down modulation, two predictions have equal probability. After top-down modulation, context contributes to favoring one unambiguous representation. **d**, model implementation of dendritic integration using a hierarchical convolutional neural network. **e**, distinct combinations of input and context used to train the top-down network g . **f**, possible combinations of input and context used during training and analysis.

associated with overlapping clusters were effectively disentangled after integrating matching contextual inputs (paired t-test, $t_{99} = 6.0293$, $p < 0.0001$ for silhouette scores between ambiguous images before and after integrating top-down inputs; Fig. 2c). These results show that our model learned to use contextual inputs provided to apical dendrites in the form of a one-hot encoding to modulate basal activity and resolve ambiguity in sensory inputs.

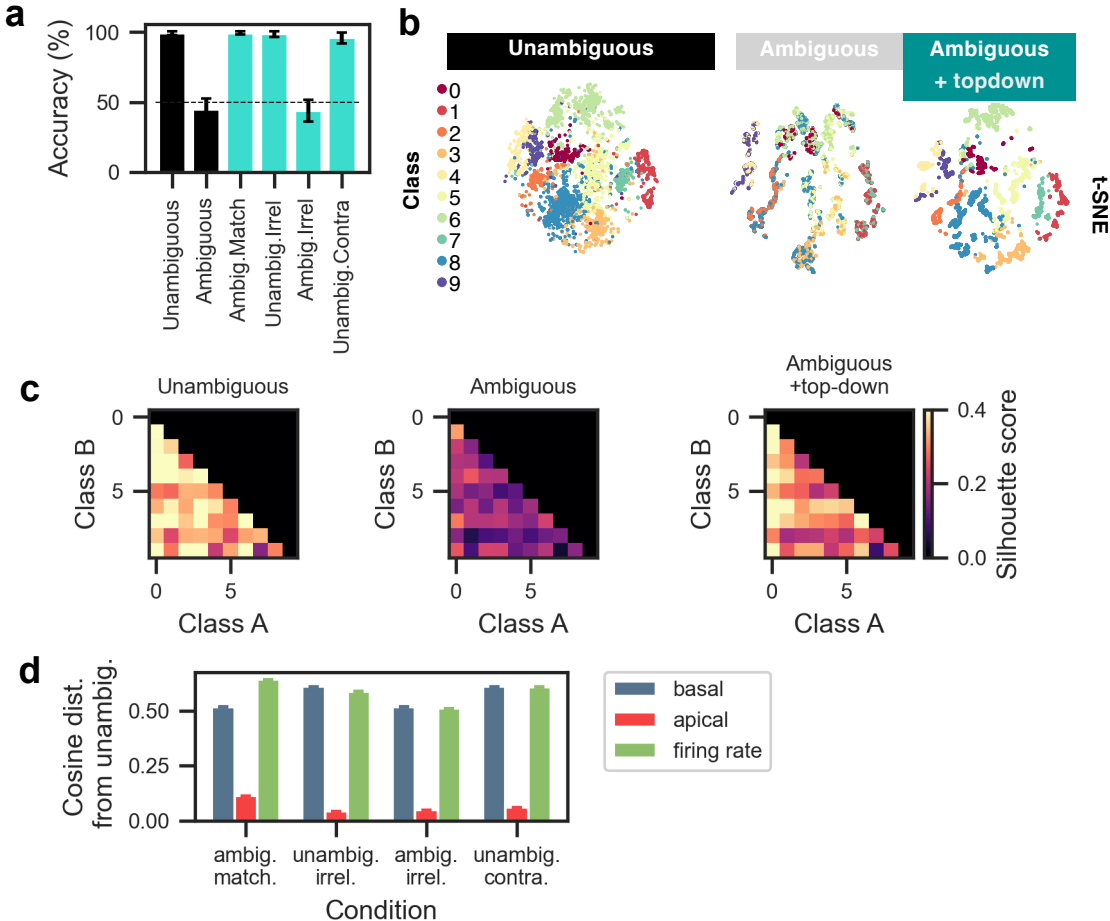


Figure 2: **Ambiguity can be resolved only when integrating top-down signals.** **a**, readout test set accuracy before and after combining top-down signals over training epochs for all input-context combinations. Dashed line corresponds to chance level. **b**, low dimensional projection (t-SNE) of h for unambiguous inputs (top), ambiguous inputs before (bottom left), and after (bottom right) top-down modulation. **c**, silhouette scores for h , for each class pair and for unambiguous inputs (left), ambiguous inputs before (center), and after (right) top-down modulation. **d**, cosine distance between h in unambiguous conditions and basal, apical compartments and firing rate in each scenario.

Next, we evaluated the importance of the bio-inspired integration rule (Hadamard) and an arithmetic sum of basal and apical activities (3a). When inputs are ambiguous and context is useful, we find that the Hadamard integration rule outperforms arithmetic summation specifically when said context is associated with high levels of certainty (represented by a context vector with values > 0.8 for the target class; RM-ANOVA, $F_8 = 53.0945$, $p = 0.0001$ for the interaction between integration rule and contextual certainty; 3b). Interestingly, when inputs were unambiguous and context contradictory, the Hadamard integration rule only outperformed arithmetic summation for lower values of contextual certainty (RM-ANOVA, $F_8 = 19.3529$, $p = 0.0023$ for the interaction between integration rule and contextual certainty; 3c).

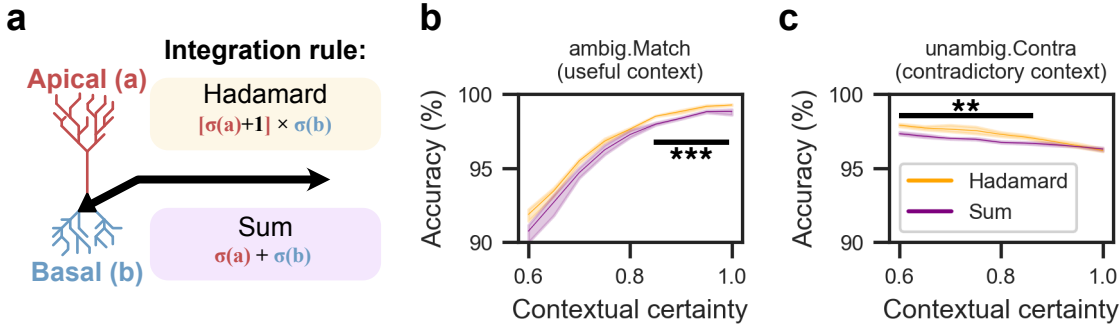


Figure 3: **Role of integration rules on ambiguity resolution.** **a**, comparison between Hadamard and arithmetic sum integration rules. **b**, test set accuracy relative to contextual certainty using either integration rule in conditions where inputs are ambiguous and context is useful. **c**, same but in conditions where inputs are unambiguous and context contradicts the true label.

2.3 Single neuron mechanisms of top-down modulation

We next sought to understand the computational role played by top-down modulation of pyramidal apical dendrites in solving this contextual integration task. To this end, we developed a method to identify neurons relevant for solving the task. We then analysed their activations across the various contextualized input conditions to reveal the differential role played by their apical compartments. First, to define the sub-populations of pyramidal neurons performing specific computations, we employed layer-wise relevance propagation (LRP; (Bach et al., 2015); supplementary Fig. 1a), a method typically used to explain which regions of an input contribute most to model output. Specifically, each neuron receives a score for its contribution to the model output for each image (Supplementary Fig. 1b). We then defined the subset of neurons most relevant for identifying a given class, S_C , as the minimum set of neurons required to account for 95% of total neuronal relevance when processing images from that class (Fig. 1c,d, see Methods). Sets of relevant neurons defined in this way exhibit low overlap between classes (Supplementary Fig. 1b-d, see Methods). We observed similar representational separability between classes for other scenario and given appropriate top-down inputs (Supplementary Fig. 1e). Additionally, these sets of relevant neurons are typically sparse and represent $\sim 15\%$ of the total neuronal population (Supplementary Fig. 1b,c).

It is noteworthy that the model is not explicitly provided with the ambiguous nature of input images, and therefore learns to extract this information to solve the task. In addition, the model learns to ignore top-down signals when the image is unambiguous and context is contradictory. Given that the apical compartment must combine contextual information and the contextually naive output differentially depending on the ambiguity of the input, we hypothesized that solving the task effectively required the modulation of a subset of neurons encoding overlapping or entangled features for each class pair. To assess this possibility, we registered the amplitude of apical signals arriving at LRP subsets pertaining to class-specific neurons and class-pair overlapping neurons in each scenario (Fig. 4a-f). When comparing all input/context scenarios, we found that apical signals were highest when input images were ambiguous and context informative (1-ANOVA, $F_{416}=237.024$, $p < 0.0001$, for the main effect of input/context scenario; Fig. 4b). Across all scenarios, neurons most relevant for class-pairs were associated with the highest amplitude in the apical compartment (1-ANOVA, $F_{417}=17.9445$, $p < 0.0001$, for the main effect of neuron class; Fig. 4b). We hypothesized that class-pair overlapping neurons are also most modulated by top-down context, and that modulating these neurons is necessary to solve the perceptual ambiguity classification task (Fig. 4c).

To evaluate this hypothesis, we applied a mask on selected neurons at inference time and assessed the model’s performance. Specifically, we assess readout test set accuracy when inputs are ambiguous and context is helpful, and compare cases where class-pair overlapping neurons (as identified with LRP) are specifically masked (by setting their value to 0) to cases where other randomly selected neurons are masked. We also evaluate the effect of mask size and found that masking class-pair overlapping neurons specifically lead to significantly more rapid degradation of accuracy with increasing mask size compared to other neurons (Fig. 4d). This highlights the key role of these neurons’ apical compartments in integrating relevant contextual signals.

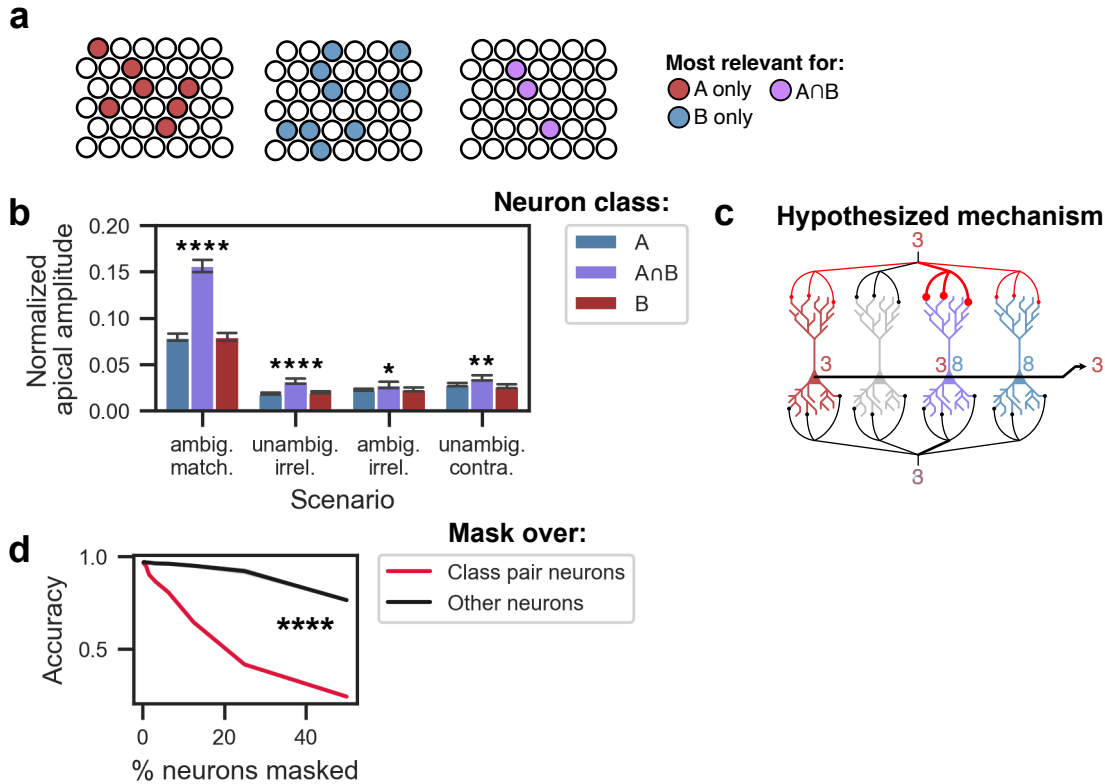


Figure 4: **Class-pair overlapping neurons receive the strongest top-down signals.** **a**, using layer-wise relevance propagation, we identify neurons most relevant for either of two classes (red and blue), or overlap of both classes (magenta). **b**, amplitude of the apical compartment (normalized over all neurons) for each input/context condition. Three distinct classes of neurons are compared: neurons most relevant for unambiguous class A (blue), B (red), or neurons most relevant for both A and B classes (magenta). **c**, we hypothesize that class-pair overlapping neurons receive the highest amplitude of top-down signals when processing ambiguous images, especially given matching context.

Task	context	ambig.Match	unambig.Match	unambig.Irrel	ambig.Irrel	unambig.Contra
MNIST	oracle	0.996 \pm 0.000	0.983 \pm 0.001	0.979 \pm 0.002	0.461 \pm 0.003	0.964 \pm 0.001
MNIST	temporal	0.963 \pm 0.001	0.999 \pm 0.000	0.991 \pm 0.001	0.487 \pm 0.005	0.990 \pm 0.001
EMNIST	oracle	0.993 \pm 0.001	0.969 \pm 0.003	0.936 \pm 0.003	0.469 \pm 0.004	0.903 \pm 0.002

Table 1: Readout test set accuracy on MNIST and EMNIST with different context representations. Results are expressed for each scenario as mean % \pm standard deviation.

2.4 Deriving context from temporal information

Contextual priors can also be extracted from the temporal domain, specifically by leveraging past information to decode incoming ambiguous sensory inputs. To extend our model to cases where contextual signals are derived from the temporal domain, we trained a Gated Recurrent Unit (GRU) network to predict the arithmetic sum of two unambiguous digits as encoded by our pretrained feedforward weights Θ_b . The final output state of the GRU was then given as a contextual signal for our model (fig. 5a; see Methods). We find that in cases where the input is ambiguous and the temporal sequence sums to a plausible interpretation of the ambiguous image, the model updates perceptual representations using contextual signals to successfully resolve ambiguities (fig. 5b, top). Importantly, context is effectively ignored in cases where input is unambiguous and contextual signals irrelevant (fig. 5b, bottom). Using low-dimensional projections of latent representations, we find that top-down context derived from the temporal domain effectively disentangled overlapping representations when inputs are ambiguous, similarly to the oracle case. (fig. 5c)

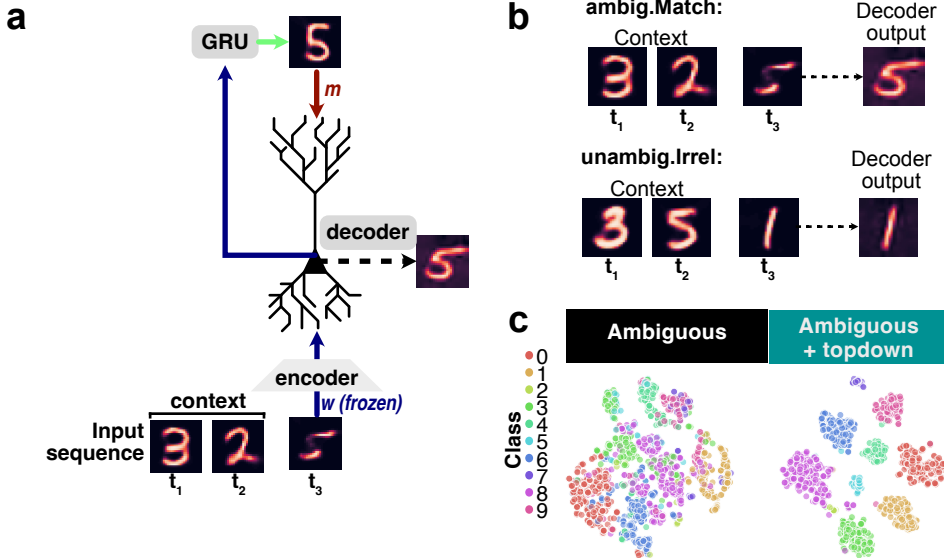


Figure 5: **Deriving context from temporal information.** **a**, rationale for training a model that leverages context derived from temporal sequences through a recurrent network (GRU). **b**, example sequence used to generate context signals (as the arithmetic sum of two digits, left and center columns) to resolve ambiguity of an input image (right column). **c**, t-SNE projection of latent representation associated with ambiguous inputs before (left) and after (right) combining top-down signals.

3 Discussion

The exact mechanism by which top-down signals exert their functional role in pyramidal neurons remains unknown. One hypothesis is that, in the neocortex, apical dendrites of pyramidal neurons integrate top-down information from higher-order regions, which in turn modulate somatic firing rate for accurate and robust perception. A computational framework that respects known biophysical

Table 2: Ablation experiments on EMNIST for the integration rule. Context only = 0 when the topdown network has access to feedforward latent $\mathbf{U}\mathbf{b}$ and c (standard case), and context only = 1 when only c is provided as input. Three modulation (integration) rules are tested: hadamard (ours), sum, and concat (see 3. Concat refers to a concatenation of 'topdown' weights on the basal weight matrix, akin to adding dendritic branches on the basal compartment.

ambig.Match	unambig.Match	unambig.Irrel	ambig.Irrel	unambig.Contra	modulation	context_only
0.989 ± 0.002	0.959 ± 0.003	0.931 ± 0.004	0.469 ± 0.003	0.841 ± 0.004	concat	0
0.794 ± 0.005	0.967 ± 0.003	0.938 ± 0.003	0.473 ± 0.004	0.903 ± 0.014	concat	1
0.993 ± 0.001	0.969 ± 0.003	0.936 ± 0.003	0.469 ± 0.004	0.903 ± 0.001	hadamard	0
0.913 ± 0.008	0.929 ± 0.004	0.901 ± 0.006	0.468 ± 0.005	0.738 ± 0.008	hadamard	1
0.994 ± 0.001	0.974 ± 0.001	0.944 ± 0.001	0.466 ± 0.007	0.920 ± 0.001	sum	0
0.792 ± 0.011	0.967 ± 0.005	0.937 ± 0.003	0.462 ± 0.013	0.904 ± 0.008	sum	1

constraints while leveraging a task that requires integrating different types of context is ideal for testing this hypothesis. Here, we present (1) a functional model of contextual integration at pyramidal neurons that relies on the biophysical properties of apical and basal dendrites, and (2) a novel image classification task and dataset using a conditional generative model. Specifically for (1), we implement a Hadamard (multiplicative elementwise) integration rule based on known biophysical properties of apical dendrites which act as gain modulators of somatic activity (M. E. Larkum et al., 2007; Waters et al., 2003). To solve (2), we train the top-down network (mapping of context onto apical dendrites) with the proposed loss function 5 by gradient descent, and assess the role of top-down signals in solving the task across 5 distinct input/context conditions. We find that the top-down network learns to refine ambiguous representations by applying sparse gain modulation to basal signals when contextual information is both available and relevant, but also learns to ignore contradictory or irrelevant contexts. This sparse selectivity is consistent with biased competition in the top-down modulation of pyramidal neurons. Our results show that it is in principle possible for local pyramidal circuits to learn a mapping of contextual representations onto their apical compartments to resolve perceptual ambiguity. Further analysis reveals that a sparse subset of class-pair overlapping neurons are preferentially gain-modulated by top-down contextual inputs, providing a candidate mechanism for how the model solves the perceptual ambiguities. This mixed selectivity could present distinct computational advantages across changing contexts (Rigotti et al., 2013).

3.1 Roles of top-down modulation

Top-down feedback is a prominent feature of the neocortical architecture for which several roles have been hypothesized. During learning, it has been proposed to act as a credit assignment signal (Bengio, 2020; Guerguiev et al., 2017; Lee et al., 2015; Meulemans et al., 2020) and/or representing predictions (A. Rao et al., 2022; R. P. N. Rao & Ballard, 1999). Besides its role in credit assignment, top-down feedback has also been proposed to support attentional processes (Lindsay, 2020) by dynamically highlighting the most relevant parts of an input, in both biological (Spratling, 2008) and artificial systems (Mittal et al., 2020), and could augment sensory processing with robustness to adversarial stimuli (Choksi et al., 2020) or integration of contextual or task information (Naumann et al., 2022; Wybo et al., 2022). Given their biophysical properties, apical dendrites are particularly well poised to integrate these top-down contextual signals, and from a computational perspective, have been shown to be useful for multitask learning (Wybo et al., 2022). Our computational framework falls into the category of updating feedforward representations. We do not exclude other hypothesized roles for top-down feedback, however their unification under one framework is outside of the scope of this work.

Extending previous work on integration of topdown contextual signals via apical and basal dendrites, we focus specifically on a task in which the model must learn to differentially integrate relevant and irrelevant contextual signals at apical dendrites for accurate perception. This reflects the reality for brains, where not all contextual signals are useful or relevant to the task at hand.

3.2 Role of dendritic integration algorithms on function

Previous models have proposed to integrate feed-forward and feedback information streams using additive (Choksi et al., 2020; Mittal et al., 2020), multiplicative (Naumann et al., 2022) rules, or both (Wybo et al., 2022). In Mittal et al. (2020), top-down signals come from past temporal context from higher-order modules, and are integrated with the feedforward stream via additive key-value attention ((Vaswani et al., 2023)). These works explore similar integration rules to ours, but the mathematical forms are not equivalent. Here we implement a Hadamard integration rule on the basis of a direct correspondence to biophysical principles. While the contextual integration task can be solved using different rules 2, under uncertainty, Hadamard integration enables the model to ignore contradictory contextual signals more efficiently compared to additive integration. Furthermore, as basal and apical signals are combined post-activation, our rule can only amplify already active neurons, unlike Wybo et al., 2022 and (Naumann et al., 2022). From an efficiency perspective, this eliminates the need to drive other neurons to fire, and uses less of the network capacity, at the cost of expressivity. It remains to be demonstrated whether our rule enables the model to perform well for more complex tasks.

3.3 Testable predictions

We find that our model can learn a non-linear mapping of top-down signals onto the apical compartment, a property that was recently described in pyramidal neurons of the visual cortex (Fişek et al., 2023). In addition to this compatibility with *in vivo* conditions, we propose several key links between experimental work and our model. Firstly, we found that under ambiguity, our model displayed a high diversity of neural responses as well as neurons that exhibit highly overlapping responses for specific class-pairs similar to *in vivo* reports that subsets of pyramidal neurons display a variety of responses given a mismatch between context and sensory evidence (Jordan & Keller, 2020; Rigotti et al., 2013). Secondly, we find that masking apical compartments of class-pair overlapping neurons decreased task performance by a significant margin, up to nearly chance level. This is in contrast with *in vivo* experiments in non-human primates showing that inhibiting higher-order regions, and effectively shifting visual cortex representations to a strictly feed-forward regime, increased performance delays but did not prevent object recognition even for challenging images (Kar & DiCarlo, 2021). Finally, our model could learn a mapping of top-down feedback to the apical compartment independent of learning contextual representations which is compatible with high-order cortical regions, including the hippocampus, learning and updating contextual representations in absence of sensory inputs and yet play a major role in memory retrieval that necessitate contextual information (Maren et al., 2013).

One key testable prediction from our model is that neurons displaying mixed-selectivity would receive the strongest top-down signals at their apical dendrites. Testing this would require first conducting a controlled contextual integration task with an animal, and identifying a population from which a high degree of overlap is observed in neural responses for multiple categories or task variables. We hypothesize that silencing the apical compartments of these neurons would impair the ambiguity resolution ability of the animal.

3.4 Limitations and outlook

While our model combines functionality with key biophysical properties of dendrites, there are some important assumptions and simplifications that need to be considered. Firstly, our model is designed to implement some key features of cortical pyramidal neurons without focusing on a specific subpopulation that make up cortical layers, including layer 2/3 and layer 5 pyramidal neurons. Here, we assume that contextual signals are provided by a neurons in a higher-order region, which would likely correspond to layer 5 output, and integrated in apical dendrites of putative layer 2/3 pyramidal neurons (Bastos et al., 2012; Schuman et al., 2021). It is noteworthy though that layer 5 neurons can also send top-down projections to the basal compartment of layer 2/3 neurons, although to a lesser extent (Harris et al., 2019).

Secondly, we use a deep learning framework that does not respect Dale’s principle: namely, synaptic weights can be either negative and positive, giving the ability of presynaptic neurons to be both excitatory and inhibitory at the same time for distinct postsynaptic neurons. Although our model ignores this principle, we apply normalization across inputs, which could in principle mimic a role of the inhibitory neurons if they are non-selective. Additionally, Dale’s principle could theoretically

be implemented to our deep learning framework with little sacrifice in performance (Cornford et al., 2021).

Our model heavily abstracts temporal dynamics that are normally observed in biological circuits. Specifically, perception is associated with ever evolving neurophysiological responses that anchor to discrete states of sensory experience. For example, in the presence of ambiguous stimuli, human subjects can oscillate between two interpretations, a phenomenon termed ‘perceptual bistability’ (Hardstone et al., 2021). During perceptual bistability, neural activity alternates between discrete states (Abeles et al., 1995; Akrami et al., 2009), following principles of continuous attractor dynamics (Daelli & Treves, 2010). In the future, our model could support more realistic temporal dynamics, which would enable the testing of a rich array of hypotheses regarding contextual integration.

In the future, we propose that our model could be extended to hierarchies of sensory modalities interacting with each other. Deep learning models that implement multi-modal interactions are an active area of research (Alayrac et al., 2022; Mustafa et al., 2022; Radford et al., 2021). In these cases, representations from each modality are mapped to a joint high dimensional space and optimized via a contrastive self-supervised training objective. These models do not have the explicit objective to resolve conflicting or contradictory information from other modalities. In this context, our framework could be extended to multi-modal self-supervised learning for more robust perception in deep neural networks. Finally, such a model could be leveraged to test specific hypotheses of contextual integration in health and disease, and in particular in cases where the physiological properties of pyramidal neurons are known to be altered (Kim et al., 2014).

4 Methods

4.1 Ambiguous dataset generation

To create the dataset for our task, we first train a conditional variational autoencoder (CVAE) on standard MNIST/EMNIST (Doersch, 2021; Sohn et al., 2015). The purpose of the CVAE in this setup is to use the learned latent space to generate images that are ambiguous between two digits. While category-free interpolation in the latent space can be done with a vanilla VAE, the CVAE approach facilitates the generation of ambiguous images conditioned on the specified categories. We then concatenate the input to the decoder (latent z) with a linear combination of one-hot vectors representing the target digits. We define an image to be ambiguous when it lies at the $50\% \pm 5\%$ decision boundary between two classes of a classifier trained on standard MNIST/EMNIST. We collect a set of images in triplets, where two images are unambiguous from unique classes y_0, y_1 , and the third is ambiguous (using our criterion) between y_0, y_1 , generated by the CVAE. This dataset format simplifies the implementation of our task setup.

4.2 Model architecture

The model consists of three components: the pretrained backbone, the readout for classification, and the topdown network. We first train a variational autoencoder with a convolutional encoder and decoder to form smooth latent representations of unambiguous characters. Once the variational autoencoder backbone is trained, its weights are frozen and a readout (MLP) is trained to classify the latent representations.

4.2.1 Oracle context

In the oracle case, top-down signals are provided in the form of a one-hot vector:

$$\mathbb{1}_y(c_i) := \begin{cases} 1, & \text{if } i = y. \\ 0, & \text{otherwise} \end{cases} \quad (4)$$

$\forall i \in 1 \dots C$ where C is the number of classes, $|\mathbf{c}| = C$.

4.2.2 Temporal context

In the temporal case, context signals were provided by a Gated Recurrent Unit (GRU) network (Cho et al., 2014). We trained a GRU with hidden state of size 128 to predict the modulo 10 sum of MNIST

digits in a sequence of two digits’. The input to the GRU at time t is not x_t , but rather $\mathbf{U}\mathbf{b}_t$, encoded by the pretrained backbone. After processing a sequence of digits (x_{t-2}, x_{t-1}) , the final output state o_t of the GRU was then used as a top-down context signal.

4.3 Training

4.3.1 Loss function

The topdown network $g(x, c|\Theta_a)$ is explicitly trained to minimize a loss function composed of a sum over the following 5 scenarios: ambiguous input with matching context (ambig.Match), unambiguous input with matching context (unambig.Match), unambiguous input with irrelevant context (unambig.Irrel), ambiguous input with irrelevant context (ambig.Irrel), and unambiguous input with contradictory context (unambig.Contra). All scenarios are therefore optimized together for every gradient update step. We use mean squared error as the loss criterion between the predicted latents (computed as in equation 2) and the target latents for each scenario. Each minibatch is sampled from dataset D , and scenarios sampled from the minibatch and set of contexts C .

$$\mathbf{L}(\Theta_a; D) = \mathbb{E}_{((x_0, y_0), x_{ambig}, (x_1, y_1)) \sim D, c_{match}, c_{irrel} \sim C} \left[\sum_{s=1}^5 \|\mu_s^* - \hat{\mu}_s\|_2^2 \right] \quad (5)$$

It should be noted that x_0, x_1 are unambiguous images sampled from D . The optimum of Θ_a is given by:

$$\Theta_a^* = \underset{\Theta_a}{\operatorname{argmin}} L(\Theta_a; D) \quad (6)$$

Here, μ_s^* is the target representation, which is for each scenario and context:

$$\mu_s^* := \begin{cases} \mathbf{U}\sigma(\mathbf{b}_{c_{match}}), & \text{if } s \in \{1\} \\ \mathbf{U}\sigma(\mathbf{b}_{unambig}), & \text{if } s \in \{2, 3, 5\} \\ \mathbf{U}\sigma(\mathbf{b}_{ambig}), & \text{if } s \in \{4\} \end{cases} \quad (7)$$

Where $b_c = f(x_c|\Theta_b)$, and $b_{unambig} = f([x_0, x_1]|\Theta_b)$. Predicted latents are given by:

$$\hat{\mu}_s := \begin{cases} \mathbf{U}\sigma(\mathbf{b}_{ambig}) \odot (\mathbf{1} + \sigma(\mathbf{a}_{b_{ambig}, c_{match}})), & \text{if } s \in \{1\} \\ \mathbf{U}\sigma(\mathbf{b}_{unambig}) \odot (\mathbf{1} + \sigma(\mathbf{a}_{b_{unambig}, c_{match}})), & \text{if } s \in \{2\} \\ \mathbf{U}\sigma(\mathbf{b}_{unambig}) \odot (\mathbf{1} + \sigma(\mathbf{a}_{b_{unambig}, c_{irrel}})), & \text{if } s \in \{3\} \\ \mathbf{U}\sigma(\mathbf{b}_{ambig}) \odot (\mathbf{1} + \sigma(\mathbf{a}_{b_{ambig}, c_{irrel}})), & \text{if } s \in \{4\} \\ \mathbf{U}\sigma(\mathbf{b}_{unambig}) \odot (\mathbf{1} + \sigma(\mathbf{a}_{b_{unambig}, c_{contra}})), & \text{if } s \in \{5\} \end{cases} \quad (8)$$

Where $\mathbf{a}_{b,c} = g(\mathbf{U}\mathbf{b}, \mathbf{c}|\Theta_a)$ (See pseudocode 1)

4.3.2 Layer-wise Relevance Propagation Analysis

We applied layer-wise relevance propagation (LRP) to identify specific neurons whose activity, as described by \mathbf{h} in our model, contributed most to the category readouts. For this analysis, we trained a readout to classify the standard categories (ie. digits 0-9) as well as all possible ambiguous pairs (ie. 3/5, 5/8, 1/7, etc.), which for MNIST gives a total number of categories $C = 55$. To identify the subset of neurons that are most relevant for a given class i , we sorted neurons by highest to lowest average relevance per class. We then computed the normalized cumulative sum of relevance of neurons, and define S_i as the minimum set of neurons required to obtained 95% of the total LRP for each class i where $i \in 0, 1, \dots, C$ (fig. 1d). We computed the separability between sets S_i, S_j as $1 - |S_i \cap S_j|/|S_i \cup S_j|$ (Fig. 1e).

4.4 Statistical analysis

Parametric tests were used when data distribution was normal and variance homogeneous, otherwise non-parametric tests were used and reported when appropriate. **Meaning of abbreviated statistical terms.** 1-ANOVA: one-way ANOVA; 2-ANOVA, two-way ANOVA; RM-ANOVA, repeated-measure ANOVA. Error bars and bands represent standard error of the mean, unless stated otherwise. *, $p < 0.05$; **, $p < 0.01$; ***, $p < 0.001$; ****, $p < 0.0001$; n.s., not significant.

Algorithm 1 Training of the top-down model with oracle context

Require: Dataset D , learning rate λ , dimension of basal activation d_b , number of classes C , top-down input \mathbb{R}^{d_b+C} , output: \mathbb{R}^{d_b} , bottom-up network (frozen) f_{Θ_b} , latent projection (frozen) \mathbf{U} , top-down network $g(\cdot; \Theta_a)$, batch size B

- 1:
- 2: $\Theta_a \leftarrow \text{init_kaiming}()$
- 3: **for** triplet minibatch $(\mathbf{x}_0, \mathbf{y}_0), (\mathbf{x}_1, \mathbf{y}_1)$ sampled from D **do**
- 4: $y \leftarrow \{\mathbf{y}_0, \mathbf{y}_1\}$
- 5: $x \leftarrow \{\mathbf{x}_0, \mathbf{x}_1\}$
- 6: # Concatenate all scenarios into single batch
- 7: $\mathbf{c}_{\text{match}} \leftarrow \text{random_choice}(y, \text{size} = B)$ # Sample context uniformly from y over minibatch
- 8: $\mathbf{c}_{\text{irrel}} \leftarrow \text{random_choice}(\text{range}(C) \setminus y, \text{size} = B)$ # Sample context uniformly (excluding S)
- 9: $\mathbf{c}_{\text{contra}} \leftarrow \mathbf{y}_1$
- 10: # combine all vectors into one for efficiency
- 11: $c \leftarrow \text{cat}(\mathbf{c}_{\text{match}}, \mathbf{c}_{\text{match}}, \mathbf{c}_{\text{irrel}}, \mathbf{c}_{\text{irrel}}, \mathbf{c}_{\text{contra}})$
- 12: $\mu^* \leftarrow \text{cat}(\mu_{\mathbf{c}_{\text{match}}}, \mu_y, \mu_y, \mu_{\text{ambig}}, \mu_{y_0})$
- 13: $x \leftarrow (x_{\text{ambig}}, x, x, x_{\text{ambig}}, x_0)$
- 14: $b \leftarrow f(x; \Theta_b)$
- 15: $a \leftarrow g(\mathbf{U}b \oplus c; \Theta_a)$
- 16: $\hat{\mathbf{h}} \leftarrow \text{relu}(b) \odot (1 + \text{relu}(a))$
- 17: $\hat{\mu} \leftarrow \mathbf{U}\hat{\mathbf{h}}$
- 18: $\text{Loss} \leftarrow \text{mse}(\hat{\mu}, \mu^*)$
- 19: # autograd optimizer step
- 20: $\Theta_a \leftarrow \Theta_a + \lambda \nabla_{\Theta_a} \text{Loss}$

4.5 Code availability

All experiments were carried out using PyTorch. We use the MNIST and EMNIST datasets, where number of output classes are $C = 10$ for MNIST, and $C = 26$ for EMNIST. The code for models and data analysis is publicly available under: <https://github.com/ABL-Lab/expectation-clamp> The code used to generate the ambiguous datasets as well as links to pre-generated datasets are available under: <https://github.com/ABL-Lab/ambiguous-dataset>

5 Acknowledgements

We thank Roberto Araya, Doina Precup, Irina Rish, and Yoshua Bengio for helpful discussions. This study was supported by funding from the Institute for Data Valorization (IVADO), the Unifying Neuroscience and Artificial Intelligence - Québec (UNIQUE) research center, the CHU Sainte-Justine Research Center (CHUSJRC), Fonds de Recherche du Québec-Santé (FRQS), the Canada CIFAR AI Chairs Program, the Quebec Institute for Artificial Intelligence (Mila), and Google. B.A.R. was supported by NSERC (Discovery Grant: RGPIN-2020-05105; Discovery Accelerator Supplement: RGPAS-2020-00031), CIFAR (Canada AI Chair; Learning in Machine and Brains Fellowship) and the Canada First Research Excellence Fund (CFREF Competition 2, 2015-2016) awarded to the Healthy Brains, Healthy Lives initiative at McGill University, through the Helmholtz International BigBrain Analytics and Learning Laboratory (HIBALL). Compute infrastructure was supported through a grant of computing time to E.B.M. from the Digital Research Alliance of Canada. N.I. received additional support from a NSERC Undergraduate student research award, and IVADO and UNIQUE excellence fellowships. M.T received additional support from the HBHL Graduate Fellowship. B.T.G. received additional support from a UNIQUE excellence fellowship.

References

- Abeles, M., Bergman, H., Gat, I., Meilijson, I., Seidemann, E., Tishby, N., & Vaadia, E. (1995). Cortical activity flips among quasi-stationary states. [Publisher: Proceedings of the National Academy of Sciences]. *Proceedings of the National Academy of Sciences*, *92*(19), 8616–8620. <https://doi.org/10.1073/pnas.92.19.8616>
- Akrami, A., Liu, Y., Treves, A., & Jagadeesh, B. (2009). Converging Neuronal Activity in Inferior Temporal Cortex during the Classification of Morphed Stimuli. *Cerebral Cortex*, *19*(4), 760–776. <https://doi.org/10.1093/cercor/bhn125>
- Alayrac, J.-B., Donahue, J., Luc, P., Miech, A., Barr, I., Hasson, Y., Lenc, K., Mensch, A., Millican, K., Reynolds, M., Ring, R., Rutherford, E., Cabi, S., Han, T., Gong, Z., Samangooei, S., Monteiro, M., Menick, J. L., Borgeaud, S., . . . Simonyan, K. (2022). Flamingo: A Visual Language Model for Few-Shot Learning. *Advances in Neural Information Processing Systems*, *35*, 23716–23736. Retrieved June 14, 2023, from https://proceedings.neurips.cc/paper_files/paper/2022/hash/960a172bc7fbf0177ccccbb411a7d800-Abstract-Conference.html
- Bach, S., Binder, A., Montavon, G., Klauschen, F., Müller, K.-R., & Samek, W. (2015). On Pixel-Wise Explanations for Non-Linear Classifier Decisions by Layer-Wise Relevance Propagation [Publisher: Public Library of Science]. *PLOS ONE*, *10*(7), e0130140. <https://doi.org/10.1371/journal.pone.0130140>
- Bastos, A. M., Usrey, W. M., Adams, R. A., Mangun, G. R., Fries, P., & Friston, K. J. (2012). Canonical Microcircuits for Predictive Coding. *Neuron*, *76*(4), 695–711. <https://doi.org/10.1016/j.neuron.2012.10.038>
- Bengio, Y. (2020, August). Deriving Differential Target Propagation from Iterating Approximate Inverses [arXiv:2007.15139 [cs, stat]]. <https://doi.org/10.48550/arXiv.2007.15139>
- Cho, K., van Merriënboer, B., Gulcehre, C., Bahdanau, D., Bougares, F., Schwenk, H., & Bengio, Y. (2014, September). Learning Phrase Representations using RNN Encoder-Decoder for Statistical Machine Translation [arXiv:1406.1078 [cs, stat]]. Retrieved October 4, 2022, from <http://arxiv.org/abs/1406.1078>
- Choksi, B., Mozafari, M., O’May, C. B., Ador, B., Alamia, A., & VanRullen, R. (2020). Brain-inspired predictive coding dynamics improve the robustness of deep neural networks. Retrieved September 15, 2023, from <https://openreview.net/forum?id=q1o2mWaOssG>
- Cornford, J., Kalajdziewski, D., Leite, M., Lamarquette, A., Kullmann, D. M., & Richards, B. (2021, April). Learning to live with Dale’s principle: ANNs with separate excitatory and inhibitory units [Pages: 2020.11.02.364968 Section: New Results]. <https://doi.org/10.1101/2020.11.02.364968>
- Daelli, V., & Treves, A. (2010). Neural attractor dynamics in object recognition. *Experimental Brain Research*, *203*(2), 241–248. <https://doi.org/10.1007/s00221-010-2243-1>
- Doersch, C. (2021, January). Tutorial on Variational Autoencoders [arXiv:1606.05908 [cs, stat]]. <https://doi.org/10.48550/arXiv.1606.05908>
- Eichenbaum, H. (2017). On the Integration of Space, Time, and Memory. *Neuron*, *95*(5), 1007–1018. <https://doi.org/10.1016/j.neuron.2017.06.036>
- Felleman, D. J., & Van Essen, D. C. (1991). Distributed Hierarchical Processing in the Primate Cerebral Cortex. *Cerebral Cortex*, *1*(1), 1–47. <https://doi.org/10.1093/cercor/1.1.1-a>
- Fişek, M., Herrmann, D., Egea-Weiss, A., Cloves, M., Bauer, L., Lee, T.-Y., Russell, L. E., & Häusser, M. (2023). Cortico-cortical feedback engages active dendrites in visual cortex [Publisher: Nature Publishing Group]. *Nature*, 1–8. <https://doi.org/10.1038/s41586-023-06007-6>
- George, D., Lehrach, W., Kansky, K., Lázaro-Gredilla, M., Laan, C., Marthi, B., Lou, X., Meng, Z., Liu, Y., Wang, H., Lavin, A., & Phoenix, D. S. (2017). A generative vision model that trains with high data efficiency and breaks text-based CAPTCHAs [Publisher: American Association for the Advancement of Science]. *Science*, *358*(6368), eaag2612. <https://doi.org/10.1126/science.aag2612>
- Gilbert, C. D., & Li, W. (2013). Top-down influences on visual processing [Number: 5 Publisher: Nature Publishing Group]. *Nature Reviews Neuroscience*, *14*(5), 350–363. <https://doi.org/10.1038/nrn3476>
- Guerguiev, J., Lillicrap, T. P., & Richards, B. A. (2017). Towards deep learning with segregated dendrites. *eLife*, *6*, e22901. <https://doi.org/10.7554/eLife.22901>

- Hardstone, R., Zhu, M., Flinker, A., Melloni, L., Devore, S., Friedman, D., Dugan, P., Doyle, W. K., Devinsky, O., & He, B. J. (2021). Long-term priors influence visual perception through recruitment of long-range feedback [Number: 1 Publisher: Nature Publishing Group]. *Nature Communications*, *12*(1), 6288. <https://doi.org/10.1038/s41467-021-26544-w>
- Harris, J. A., Mihalas, S., Hirokawa, K. E., Whitesell, J. D., Choi, H., Bernard, A., Bohn, P., Caldejon, S., Casal, L., Cho, A., Feiner, A., Feng, D., Gaudreault, N., Gerfen, C. R., Graddis, N., Groblewski, P. A., Henry, A. M., Ho, A., Howard, R., . . . Zeng, H. (2019). Hierarchical organization of cortical and thalamic connectivity [Number: 7781 Publisher: Nature Publishing Group]. *Nature*, *575*(7781), 195–202. <https://doi.org/10.1038/s41586-019-1716-z>
- Jarvis, S., Nikolic, K., & Schultz, S. R. (2018). Neuronal gain modulability is determined by dendritic morphology: A computational optogenetic study [Publisher: Public Library of Science]. *PLoS Computational Biology*, *14*(3), e1006027. <https://doi.org/10.1371/journal.pcbi.1006027>
- Jordan, R., & Keller, G. B. (2020). Opposing Influence of Top-down and Bottom-up Input on Excitatory Layer 2/3 Neurons in Mouse Primary Visual Cortex. *Neuron*, *108*(6), 1194–1206.e5. <https://doi.org/10.1016/j.neuron.2020.09.024>
- Kar, K., & DiCarlo, J. J. (2021). Fast Recurrent Processing via Ventrolateral Prefrontal Cortex Is Needed by the Primate Ventral Stream for Robust Core Visual Object Recognition. *Neuron*, *109*(1), 164–176.e5. <https://doi.org/10.1016/j.neuron.2020.09.035>
- Kim, M., Kim, S. N., Lee, S., Byun, M. S., Shin, K. S., Park, H. Y., Jang, J. H., & Kwon, J. S. (2014). Impaired mismatch negativity is associated with current functional status rather than genetic vulnerability to schizophrenia. *Psychiatry Research: Neuroimaging*, *222*(1), 100–106. <https://doi.org/10.1016/j.psychres.2014.02.012>
- Larkum, M. (2013). A cellular mechanism for cortical associations: An organizing principle for the cerebral cortex [Publisher: Elsevier]. *Trends in Neurosciences*, *36*(3), 141–151. <https://doi.org/10.1016/j.tins.2012.11.006>
- Larkum, M. E., Senn, W., & Lüscher, H.-R. (2004). Top-down Dendritic Input Increases the Gain of Layer 5 Pyramidal Neurons. *Cerebral Cortex*, *14*(10), 1059–1070. <https://doi.org/10.1093/cercor/bhh065>
- Larkum, M. E., Zhu, J. J., & Sakmann, B. (1999). A new cellular mechanism for coupling inputs arriving at different cortical layers [Number: 6725 Publisher: Nature Publishing Group]. *Nature*, *398*(6725), 338–341. <https://doi.org/10.1038/18686>
- Larkum, M. E., Waters, J., Sakmann, B., & Helmchen, F. (2007). Dendritic Spikes in Apical Dendrites of Neocortical Layer 2/3 Pyramidal Neurons [Publisher: Society for Neuroscience Section: Articles]. *Journal of Neuroscience*, *27*(34), 8999–9008. <https://doi.org/10.1523/JNEUROSCI.1717-07.2007>
- Lee, D.-H., Zhang, S., Fischer, A., & Bengio, Y. (2015). Difference Target Propagation. In A. Appice, P. P. Rodrigues, V. Santos Costa, C. Soares, J. Gama, & A. Jorge (Eds.), *Machine Learning and Knowledge Discovery in Databases* (pp. 498–515). Springer International Publishing. https://doi.org/10.1007/978-3-319-23528-8_31
- Lindsay, G. W. (2020). Attention in Psychology, Neuroscience, and Machine Learning. *Frontiers in Computational Neuroscience*, *14*. Retrieved June 22, 2022, from <https://www.frontiersin.org/article/10.3389/fncom.2020.00029>
- Maaten, L. (2008). Visualizing data using t-SNE. *Journal of Machine Learning Research*, *9*(Nov), 2579. Retrieved August 31, 2023, from <https://cit.rii.ac.jp/crid/1370567187575316229>
- Maren, S., Phan, K. L., & Liberzon, I. (2013). The contextual brain: Implications for fear conditioning, extinction and psychopathology [Number: 6 Publisher: Nature Publishing Group]. *Nature Reviews Neuroscience*, *14*(6), 417–428. <https://doi.org/10.1038/nrn3492>
- Markov, N. T., Vezoli, J., Chameau, P., Falchier, A., Quilodran, R., Huissoud, C., Lamy, C., Misery, P., Giroud, P., Ullman, S., Barone, P., Dehay, C., Knoblauch, K., & Kennedy, H. (2014). Anatomy of hierarchy: Feedforward and feedback pathways in macaque visual cortex [eprint: <https://onlinelibrary.wiley.com/doi/pdf/10.1002/cne.23458>]. *Journal of Comparative Neurology*, *522*(1), 225–259. <https://doi.org/10.1002/cne.23458>
- Meulemans, A., Carzaniga, F., Suykens, J., Sacramento, J., & Grewe, B. F. (2020). A Theoretical Framework for Target Propagation. *Advances in Neural Information Processing Systems*, *33*, 20024–20036. Retrieved September 13, 2022, from <https://proceedings.neurips.cc/paper/2020/hash/e7a425c6ece20cbc9056f98699b53c6f-Abstract.html>

- Mittal, S., Lamb, A., Goyal, A., Voleti, V., Shanahan, M., Lajoie, G., Mozer, M., & Bengio, Y. (2020). Learning to Combine Top-Down and Bottom-Up Signals in Recurrent Neural Networks with Attention over Modules [ISSN: 2640-3498]. *Proceedings of the 37th International Conference on Machine Learning*, 6972–6986. Retrieved October 19, 2022, from <https://proceedings.mlr.press/v119/mittal20a.html>
- Mumford, D. (1992). On the computational architecture of the neocortex. *Biological Cybernetics*, 66(3), 241–251. <https://doi.org/10.1007/BF00198477>
- Mustafa, B., Riquelme, C., Puigcerver, J., Jenatton, R., & Hounsby, N. (2022). Multimodal Contrastive Learning with LIMoE: The Language-Image Mixture of Experts. *Advances in Neural Information Processing Systems*, 35, 9564–9576. Retrieved August 31, 2023, from https://proceedings.neurips.cc/paper_files/paper/2022/hash/3e67e84abf900bb2c7cbd5759bfce62d-Abstract-Conference.html
- Nassi, J. J., Lomber, S. G., & Born, R. T. (2013). Corticocortical Feedback Contributes to Surround Suppression in V1 of the Alert Primate. *Journal of Neuroscience*, 33(19), 8504–8517. <https://doi.org/10.1523/JNEUROSCI.5124-12.2013>
- Naumann, L. B., Keijsers, J., & Sprekeler, H. (2022). Invariant neural subspaces maintained by feedback modulation (S. Ostojic & A. J. King, Eds.) [Publisher: eLife Sciences Publications, Ltd]. *eLife*, 11, e76096. <https://doi.org/10.7554/eLife.76096>
- Radford, A., Kim, J. W., Hallacy, C., Ramesh, A., Goh, G., Agarwal, S., Sastry, G., Askell, A., Mishkin, P., Clark, J., Krueger, G., & Sutskever, I. (2021, February). Learning Transferable Visual Models From Natural Language Supervision [arXiv:2103.00020 [cs] version: 1]. <https://doi.org/10.48550/arXiv.2103.00020>
- Rao, A., Legenstein, R., Subramoney, A., & Maass, W. (2022, June). Self-supervised learning of probabilistic prediction through synaptic plasticity in apical dendrites: A normative model [Pages: 2021.03.04.433822 Section: New Results]. <https://doi.org/10.1101/2021.03.04.433822>
- Rao, R. P. N., & Ballard, D. H. (1999). Predictive coding in the visual cortex: A functional interpretation of some extra-classical receptive-field effects [Number: 1 Publisher: Nature Publishing Group]. *Nature Neuroscience*, 2(1), 79–87. <https://doi.org/10.1038/4580>
- Rigotti, M., Barak, O., Warden, M. R., Wang, X.-J., Daw, N. D., Miller, E. K., & Fusi, S. (2013). The importance of mixed selectivity in complex cognitive tasks [Number: 7451 Publisher: Nature Publishing Group]. *Nature*, 497(7451), 585–590. <https://doi.org/10.1038/nature12160>
- Schuman, B., Dellal, S., Prönnke, A., Machold, R., & Rudy, B. (2021). Neocortical Layer 1: An Elegant Solution to Top-Down and Bottom-Up Integration [eprint: <https://doi.org/10.1146/annurev-neuro-100520-012117>]. *Annual Review of Neuroscience*, 44(1), 221–252. <https://doi.org/10.1146/annurev-neuro-100520-012117>
- Sherman, S. M., & Guillery, R. W. (1998). On the actions that one nerve cell can have on another: Distinguishing “drivers” from “modulators” [Publisher: Proceedings of the National Academy of Sciences]. *Proceedings of the National Academy of Sciences*, 95(12), 7121–7126. <https://doi.org/10.1073/pnas.95.12.7121>
- Sohn, K., Lee, H., & Yan, X. (2015). Learning Structured Output Representation using Deep Conditional Generative Models. *Advances in Neural Information Processing Systems*, 28. Retrieved December 1, 2022, from <https://proceedings.neurips.cc/paper/2015/hash/8d55a249e6baa5c06772297520da2051-Abstract.html>
- Spoerer, C. J., McClure, P., & Kriegeskorte, N. (2017). Recurrent Convolutional Neural Networks: A Better Model of Biological Object Recognition. *Frontiers in Psychology*, 8. Retrieved August 2, 2022, from <https://www.frontiersin.org/articles/10.3389/fpsyg.2017.01551>
- Spratling, M. (2008). Reconciling predictive coding and biased competition models of cortical function. *Frontiers in Computational Neuroscience*, 2. Retrieved August 31, 2023, from <https://www.frontiersin.org/articles/10.3389/neuro.10.004.2008>
- Spruston, N. (2008). Pyramidal neurons: Dendritic structure and synaptic integration. *Nature Reviews Neuroscience*, 9(3), 206–221. <https://doi.org/10.1038/nrn2286>
- Stuart, G., & Spruston, N. (1998). Determinants of Voltage Attenuation in Neocortical Pyramidal Neuron Dendrites [Publisher: Society for Neuroscience Section: ARTICLE]. *Journal of Neuroscience*, 18(10), 3501–3510. <https://doi.org/10.1523/JNEUROSCI.18-10-03501.1998>

- Vaswani, A., Shazeer, N., Parmar, N., Uszkoreit, J., Jones, L., Gomez, A. N., Kaiser, L., & Polosukhin, I. (2023, August). Attention Is All You Need [arXiv:1706.03762 [cs]]. Retrieved September 13, 2023, from <http://arxiv.org/abs/1706.03762>
- Wang, C., Waleszczyk, W. J., Burke, W., & Dreher, B. (2007). Feedback signals from cat's area 21a enhance orientation selectivity of area 17 neurons. *Experimental Brain Research*, *182*(4), 479–490. <https://doi.org/10.1007/s00221-007-1014-0>
- Waters, J., Larkum, M., Sakmann, B., & Helmchen, F. (2003). Supralinear Ca²⁺ Influx into Dendritic Tufts of Layer 2/3 Neocortical Pyramidal Neurons In Vitro and In Vivo [Publisher: Society for Neuroscience Section: Cellular/Molecular]. *Journal of Neuroscience*, *23*(24), 8558–8567. <https://doi.org/10.1523/JNEUROSCI.23-24-08558.2003>
- Wybo, W. A., Tsai, M. C., Khoa Tran, V. A., Illing, B., Jordan, J., Morrison, A., & Senn, W. (2022, November). *Dendritic modulation enables multitask representation learning in hierarchical sensory processing pathways* (preprint). Neuroscience. <https://doi.org/10.1101/2022.11.25.517941>

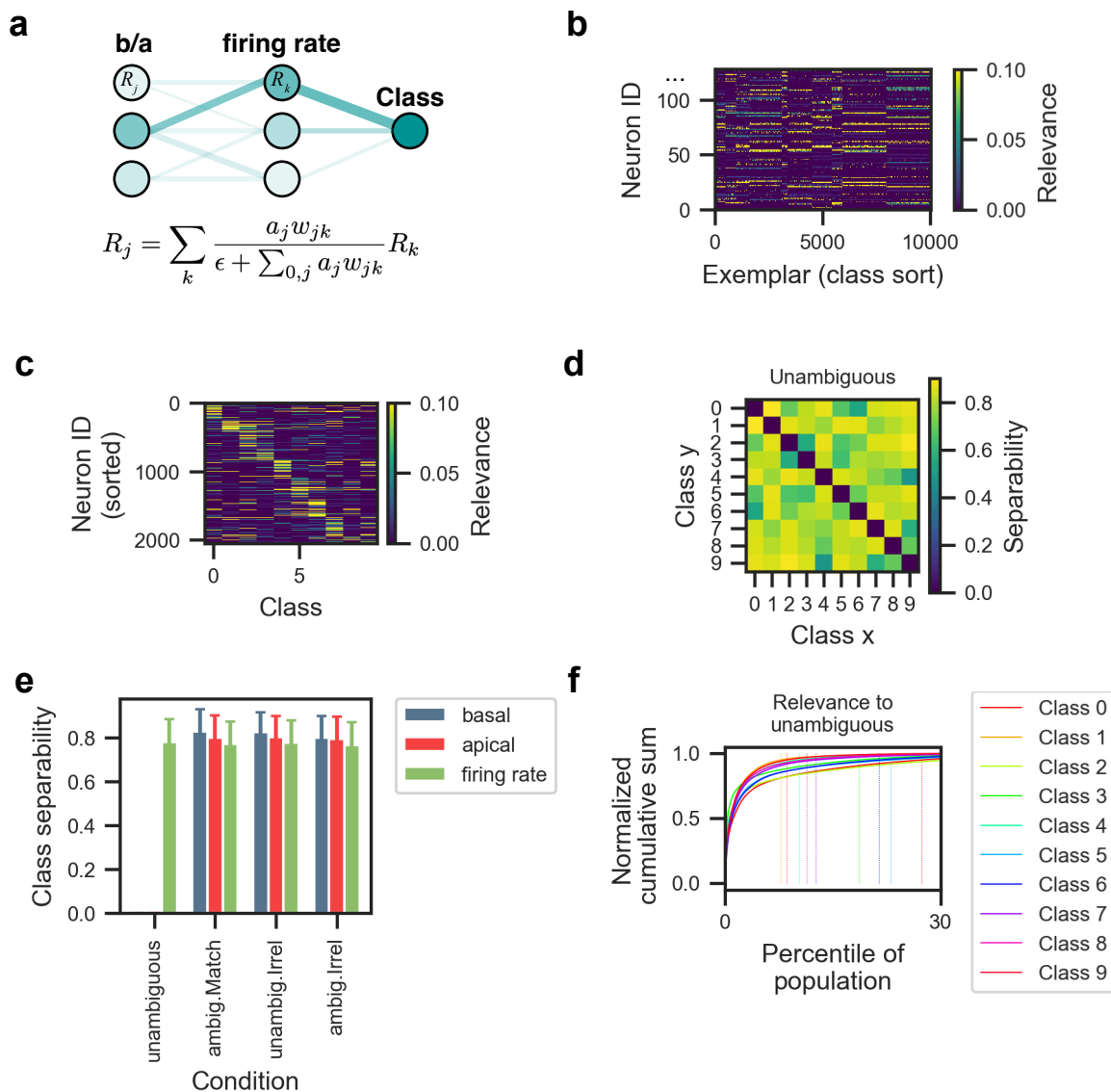


Figure 1: **Rationale for identification of single neuron groups.** **a**, we computed relevance of neurons and their compartments (basal, apical, firing rate) using LRP. **b**, Relevance of each neuron (soma) for input images sorted by class label. **c**, average relevance for each neurons (ascending sort) for each class. **d**, representational separability for every pair of classes. **e**, class separability for each training scenario, and per dendritic compartment (blue, basal; red, apical; green, firing rate). **f**, normalized cumulative sum of relevance for ranked neurons and for each class. Vertical dashed lines indicate the minimum number of neurons required to preserve 95% of all relevance for each class.